The ISME Journal (2012) 6, 1018–1031

www.nature.com/ismej

ORIGINAL ARTICLE

Anaerobic oxidation of methane at different temperature regimes in Guaymas Basin hydrothermal sediments

Jennifer F Biddle[1], Zena Cardman[2], Howard Mendlovitz[2], Daniel B Albert[2], Karen G Lloyd[2,4], Antje Boetius[3] and Andreas Teske[2]

[1]*School of Marine Science and Policy, University of Delaware, Lewes, DE, USA;* [2]*Department of Marine Sciences, University of North Carolina at Chapel Hill, Chapel Hill, NC, USA and* [3]*HGF MPG Research Group for Deep Sea Ecology and Technology, Max Planck Institute for Marine Microbiology, Bremen, Germany*

Anaerobic oxidation of methane (AOM) was investigated in hydrothermal sediments of Guaymas Basin based on $\delta^{13}C$ signatures of CH_4, dissolved inorganic carbon and porewater concentration profiles of CH_4 and sulfate. Cool, warm and hot *in-situ* temperature regimes (15–20 °C, 30–35 °C and 70–95 °C) were selected from hydrothermal locations in Guaymas Basin to compare AOM geochemistry and 16S ribosomal RNA (rRNA), *mcrA* and *dsrAB* genes of the microbial communities. 16S rRNA gene clone libraries from the cool and hot AOM cores yielded similar archaeal types such as Miscellaneous Crenarchaeotal Group, Thermoproteales and anaerobic methane-oxidizing archaea (ANME)-1; some of the ANME-1 archaea formed a separate 16S rRNA lineage that at present seems to be limited to Guaymas Basin. Congruent results were obtained by *mcrA* gene analysis. The warm AOM core, chemically distinct by lower porewater sulfide concentrations, hosted a different archaeal community dominated by the two deep subsurface archaeal lineages Marine Benthic Group D and Marine Benthic Group B, and by members of the Methanosarcinales including ANME-2 archaea. This distinct composition of the methane-cycling archaeal community in the warm AOM core was confirmed by *mcrA* gene analysis. Functional genes of sulfate-reducing bacteria and archaea, *dsrAB*, showed more overlap between all cores, regardless of the core temperature. 16S rRNA gene clone libraries with Euryarchaeota-specific primers detected members of the *Archaeoglobus* clade in the cool and hot cores. A V6-tag high-throughput sequencing survey generally supported the clone library results while providing high-resolution detail on archaeal and bacterial community structure. These results indicate that AOM and the responsible archaeal communities persist over a wide temperature range.

The ISME Journal (2012) **6,** 1018–1031; doi:10.1038/ismej.2011.164; published online 17 November 2011
Subject Category: microbial ecology and functional diversity of natural habitats
Keywords: anaerobic methane oxidation; Guaymas Basin; hydrothermal vents; thermophiles

Introduction

Sulfate-dependent, anaerobic oxidation of methane (AOM) is a pervasive process in marine sediments (Reeburgh, 2007), thought to be carried out by specialized groups of anaerobic methane-oxidizing (ANME) archaea (Knittel and Boetius, 2009). The methane-rich hydrothermal sediments of Guaymas Basin, a thickly sedimented spreading center in the Gulf of California, was the first hydrothermal vent habitat where evidence for AOM was detected (Teske *et al.*, 2002). Here, the surficial layers (0–2 cm) of hydrothermally active sediments yielded 16S ribosomal RNA (rRNA) genes of ANME-1 archaea, in conjunction with characteristically $\delta^{13}C$-depleted ANME-affiliated lipids in high concentrations (Teske *et al.*, 2002). Steep temperature gradients extend from 2 °C to 20 °C at the surface downward to >100 °C at approximately 30 cm sediment depth, and select for increasingly thermophilic and hyperthermophilic microbial populations. For example, temperature optima of microbial sulfate reduction shift downcore toward the thermophilic and hyperthermophilic range (Jørgensen *et al.*, 1990; Elsgaard *et al.*, 1994), while overall rates decrease; sulfate reduction was not reliably detected at temperatures >100 °C (Weber and Jørgensen, 2002). A similarly wide temperature range might apply to AOM; this process is generally considered typical for cool marine sediments (Knittel and Boetius, 2009). Low rates of AOM have been measured in *ex-situ* high-pressure/high-temperature incubations with Guaymas Basin sediments, but

Correspondence: A Teske, Department of Marine Science, University of North Carolina at Chapel Hill, CB 3300, Chapel Hill, NC 27599 USA.
E-mail: teske@email.unc.edu
[4]Current address: Center for Geomicrobiology, Aarhus University, Aarhus, Denmark.
Received 17 May 2011; revised 2 October 2011; accepted 3 October 2011; published online 17 November 2011

without molecular identification of the active microbial populations (Kallmeyer and Boetius, 2004). Structurally diagnostic lipids for hyperthermophilic and methanotrophic archaea (glycerol dibiphytanyl glycerol tetraethers) decreased by one to three orders of magnitude towards higher temperatures at 10-15 cm sediment depth (Schouten *et al.*, 2003). So far, thermophilic, aerobic methane-oxidizing bacteria have been isolated from terrestrial hot springs (Islam *et al.*, 2008).

These results suggest potential for thermophilic AOM communities in Guaymas Basin hydrothermal sediments. Here, we present stable carbon isotopic signatures, geochemical porewater profiles and sequencing surveys of hydrothermal sediments in Guaymas Basin that indicate active AOM and ANME archaea coinciding with *in-situ* temperatures up to at least 60–70 °C. Sediment layers where anaerobic methane oxidation takes place under increasingly hot temperature regimes are identified by $\delta^{13}C$ analysis and concentration profiles of porewater methane and dissolved inorganic carbon (DIC). In these sediment horizons, Guaymas-specific lineages of ANME-1 archaea and sulfate-reducing bacteria are detected by sequencing of 16S rRNA genes and functional genes (*mcrA, dsrAB*), by pyrosequencing of archaeal and bacterial V6-tag fragments, and by sequencing of extracted and reverse-transcribed 16S rRNA. The results show how *in-situ* temperature and porewater regimes control microbial community composition in Guaymas hydrothermal sediments.

Materials and methods

Sampling and in-situ *temperature measurements*
Sediment push cores from Guaymas Basin were harvested with Submersible Alvin on dives no. 4483, 4486 and 4489 (7, 9 and 13 December 2008) at 2000 m depth. The sediments in dives 4483 and 4489 were covered with white *Beggiatoa* mats. The sampling location of dive 4483 was near a hydrothermal mound overgrown with microbial mats and *Riftia* clusters, named Mat Mound and located at 27°N00.388, 111°W24.560 (Supplementary Figure S1A). Approximately 200 m north, the sampling target of dive 4486 was located at the edge of an extensive and very hot hydrocarbon-rich sediment covered with a microbial mat area of 5–10 m diameter, named Megamat, at 27°N00.464, 111°W24.512 (Supplementary Figure S1B). Approximately 30 m southwest of the Megamat sampling location, a smaller, orange and white *Beggiatoa* mat of approximately 1 m diameter, named UNC Mat, was sampled during dive 4489 at position 27°N0.445, 111°W24.530 (Supplementary Figure S1C). For every sampling site, a temperature profile was measured with the external heat flow temperature probe of Alvin, which records temperatures at five measurement intervals, each 10 cm apart. The *in-situ* temperature gradient was measured in 5 cm depth intervals, by initially inserting the probe incompletely into the sediment so that it the upper temperature point remained 5 cm above the sediment water interface, and after this temperature reading inserting the probe fully so that the upper temperature sensor was now positioned at the sediment/water interface. On the basis of these temperature profiles, the Mat Mound, Megamat and UNC mat cores were identified as representatives for cool, warm and hot temperature regimes, respectively (Figure 1). After completing the temperature measurements, separate cores destined for measurements of geochemistry or molecular biology were taken adjacent to each other next to the temperature gradients, using the 45 cm polycarbonate push cores of Alvin with 6.25 cm interior diameter. The geochemistry cores were numbered 4483-23, 4486-24 and 4489-11; the adjacent molecular biology cores are 4483-21, 4486-22 and 4489-10 (Supplementary Figure S1). The sediment cores were returned to the ship within 2–4 h of sampling, and subsampled for molecular and geochemical analysis within 4–10 h after being kept at 4 °C. The molecular biology cores were subsampled at 2 cm depth intervals and immediately frozen in falcon tubes in liquid nitrogen shipboard. The samples remained at −80 °C until arrival in Chapel Hill, NC, USA.

Geochemical porewater analyses
Methane was analyzed by headspace analysis of subsamples of sediment placed in serum bottles with 0.1 M sodium hydroxide. Methane concentration in the headspace was quantified using standard gas chromatography using flame ionization detection. For other analyses, porewater was obtained by centrifugation of approximately 50 ml sediment samples. The supernatant was withdrawn and filtered through 0.2 μm syringe filters. Dissolved organic acids were analyzed via high-performance liquid chromatography as described previously (Martens, 1990; Albert and Martens, 1997). The stable isotopic composition of methane and DIC was determined by GC/C/IRMS using a Hewlett Packard 5890 GC coupled to a Finnegan Mat 252 Isotope Ratio Mass Spectrometer (Hewlett Packard, Wilmington, DE, USA). For sulfate measurements, plastic 15 ml tubes filled completely with sediment were centrifuged and the resulting porewater was filtered at 0.2 μm. A 1 ml subsample was acidified with 50 μl of 50% HCl and bubbled with nitrogen for 4 min to remove sulfide. Sulfate analyses were measured shipboard using a 2010i Dionex Ion Chromatograph (Sunnyvale, CA, USA) using $Ag+$ cation exchange columns (Dionex) to remove added $Cl-$ ions as previously described (Martens *et al.*, 1999). A separate 1 ml porewater subsample was drawn into a syringe containing 0.1 ml of 0.1 M zinc acetate solution to preserve the sulfide as zinc sulfide until analyzed. Sulfide was analyzed spectrophotometrically aboard the ship (Cline, 1969).

DNA/RNA extraction from sediments
Total genomic DNA was extracted from sediments using MoBio Laboratories, Inc. (Carlsbad, CA, USA)

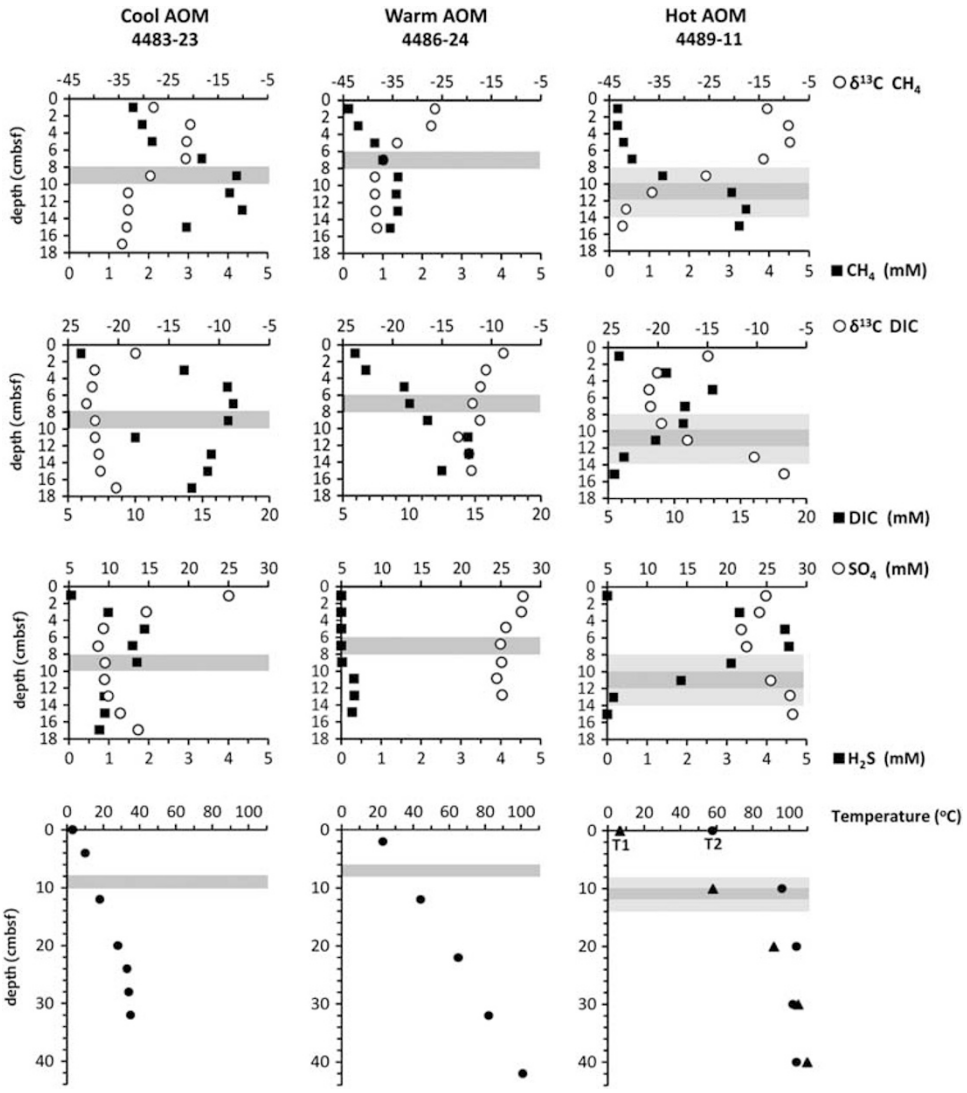

Figure 1 Compilation of geochemical profiles for Guaymas Basin sediment cores with cool, warm and hot temperature regimes. From top to bottom, the rows show methane porewater concentrations (black squares) and $\delta^{13}C$ profiles (white circles); DIC porewater concentrations (black squares) and $\delta^{13}C$ profiles (white circles); sulfide (black squares) and sulfate (white circles) porewater concentration profiles; and *in-situ* temperature profiles determined with the Alvin heatflow probe. The grey-shaded sediment layers were used for DNA and RNA extraction, and cloning and sequencing from adjacent molecular biology cores; they correspond to temperature regimes of 15–20 °C at the cool Mat Mound cores, 30–35 °C at the warm Megamat cores and 60–95 °C at the hot UNC mat cores. The additional lighter-shaded sediment layers in the hot core (8 to 10 cm and 12 to 14 cm depth) were used for amplification of *mcrA* genes, in addition to *mcrA* genes from 10 to 12 cm depth.

PowerSoil DNA Kit. RNA was extracted using the MoBio PowerSoil RNA kit (MoBio Inc.), following the manufacturer's instructions. Approximately, 0.5 (DNA) or 2.0 (RNA) grams of sediment was added to the bead tubes and the protocol was followed with one exception: the fast prep bead beater (Bio101 Thermo Savant FP120, Qbiogene, Inc., Carlsbad, CA, USA) was used to lyse the cells. DNA was extracted from cool core 4483-21, warm core 4486-22 and hot core 4489-10, at depth intervals of 8–10, 6–8 and 10–12 cm, respectively. DNA extractions from additional core 4489-10 depth sections 8–10 and 12–14 cm were also performed. RNA was extracted from sediment core 4489-10, depth 10-12 cm, using the MoBio RNA PowerSoil Total RNA Isolation Kit, following the manufacturer's instructions.

PCR amplification of 16S rRNA genes

Archaeal 16S rRNA genes were amplified using primer combinations A8f and A1492r (Teske *et al.*, 2002). Euryarchaeotal 16S rRNA genes were amplified using primers A8F and EURY498r (Burggraff *et al.*, 1994). All PCR reactions were run in a Bio-Rad iCycler Thermal Cycler machine (Hercules, CA, USA). DNA extracts were amplified using primers specified in Supplementary Table S1A. Each PCR reaction contained 1–5 μl DNA template, 2.5 μl 10 × FB1 Buffer (TaKaRa, Clontech Laboratories, Inc., Mountain View, CA, USA), 2.0 μl dNTP (2.5 mM), 2.0 μl forward-primer (10 μM), 2.0 μl reverse-primer (10 μM), 0.25 μl SpeedStar Taq polymerase (TaKaRa) and sterile H_2O to make up a 25 μl reaction. Each archaeal 16S rRNA gene PCR amplification consisted of an initial

denaturation step for 1 min at 94 °C, followed by 30 cycles consisting of 10 sec denaturation at 94 °C, 15 sec primer annealing at the annealing temperature specific for each primer combination (Supplementary Table S1A) and 20 sec of elongation at 72 °C; the amplification was concluded with an additional 1 min elongation step at 72 °C.

PCR amplification of functional genes

The two previously published primer combinations MCRf and MCRr, and ME1 and ME2 for methanogen *mcrA* genes (Springer *et al.*, 1995; Hales *et al.*, 1996) were used in a nested sequence (Supplementary Table S1B). To target methanogens and ANMEs specifically, *mcrA* and ANME-1-specific *mcrA* genes were amplified in a touchdown protocol, with primers MCR-IRDf/MCR-IRDr and ANME-1-MCRf/ANME-1-MCRr, respectively (Lever, 2008). PCR reactions were prepared as described above. For nested PCR amplifications, 0.5 to 2.0 µl of PCR product from the initial reaction was used in a subsequent 25-cycle amplification. For touchdown reactions, the initial amplification was carried out for 15 cycles, with the initial annealing temperature 5 °C warmer than the final annealing temperature listed in Supplementary Table S1A (decreasing 0.3 ° per cycle), followed by an additional 30 cycle amplification before the final elongation step. All sediment layers that were examined by 16S rRNA sequencing were also analyzed by *mcrA* gene sequencing; in some cases, nested amplification was necessary to obtain PCR amplicons of *mcrA* genes (Supplementary Table S1B). To better characterize the methane-cycling archaeal community in the hot core, we also examined additional *mcrA* genes from the sediment sections directly above (8–10 cm) and below (12–14 cm) the zone of the strongest isotopic signal indicative of AOM (10–12 cm). To target sulfate reducers, *dsrAB* genes were amplified using primer combination dsr1f/dsr4r for a 1.9 kb fragment of the *dsrAB* genes (Wagner *et al.*, 1998), followed by a nested reamplification with internal primers 1f1/1r1 as described previously (Dhillon *et al.*, 2003).

Reverse transcriptase (RT)-PCR amplification of 16S rRNA

RNA was transcribed into complementary DNA using the Takara OneStep RT-PCR kit Version 2.0 with primers A8F-A1492R (Teske *et al.*, 2002). Reagents from the TaKaRa Real Time One-Step RNA PCR Kit Ver. 2.0 were used. Each RT-PCR reaction contained 12.5 µl RT-PCR buffer 1 (TaKaRa), 2.0 µl 10 µM forward-primer, 10 µM reverse-primer, 0.5 µl RNase inhibitor (TaKaRa), 0.5 µl ExTaq polymerase (TaKaRa), reverse transcriptase (TaKaRa) and sterile H_2O to make a 25 µl reaction. Conditions for RT-PCR in a Bio-Rad iCycler were as follows: reverse transcription at 50 °C for 10 min, reverse transcriptase inactivation and HotStar Taq activation at 95 °C for 2 min, followed by 25 cycles for archaeal 16S rRNA complementary DNA, each consisting of 20 sec of denaturation at 98 °C, 15sec primer annealing at primer annealing temperature (Supplementary Table S1a) and 20 sec of elongation at 72 °C. A control reaction with no reverse transcriptase was amplified to demonstrate the absence of DNA contamination.

Cloning and sequencing of PCR-amplified 16S rRNA genes and functional genes

PCR products were gel purified using the Promega Wizard SV Gel and PCR Clean-Up System, following the manufacturer's instructions (Promega Corp., Madison, WI, USA). PCR products were ligated into pCR 2.1 TOPO Cloning Vector and transformed into chemically competent TOP-10 *Escherichia coli* cells using the TOPO TA Cloning Kit (Invitrogen, Inc., Carlsbad, CA, USA). Transformants were plated onto LB/Xgal/Kanamycin plates and incubated at 37 °C overnight. White colonies were picked and re-plated for sequencing (GENEWIZ, Inc., South Plainfield, NJ, USA) using vector-based M13F/R priming sites.

Sequence analysis

Sequences were analyzed and contigs were constructed as needed in Sequencher (Genecodes, Inc., Gene Codes, Inc., Ann Arbor, MI, USA). Chimeric 16S rRNA gene sequences were identified using Bellerophon software of Greengenes (http://greengenes.lbl.gov), or by visual inspection of ARB alignments and discarded from further analyses. Sequences were initially analyzed using BLAST (http://www.ncbi.nlm.nih.gov/BLAST/). Phylogenetic assignments of 16S rRNA and functional genes were made by creating alignments and distance-based neighbor-joining phylogenies for all sequence data sets in the ARB software platform (www.arb-home.de), and tested with 1000 bootstrap reiterations in ARB (Ludwig *et al.*, 2004), and in PAUP*4.0b (Swofford, 2000) for the Supplementary trees. Sequences have been deposited in the GenBank archive under accession numbers: JF937715–JF937796 for 16S rRNA gene sequences, JF937797–JF937831 for *mcrA* gene sequences, and JF937832– JF937857 for *dsrAB* gene sequences.

V6 tagged sequencing

DNA from the extracts described above were analyzed by V6-tag 454 pyrosequencing on a Roche GS20 at the Josephine Bay Paul Center at the Marine Biological Laboratory, (Woods Hole, MA, USA). Using the methods of the International Census of Marine Microbes (ICoMM), the variable 6 (V6) region of bacterial and archaeal 16S rRNA genes (positions 958F/1048R for archaea, and 967F/1046R for bacteria) was amplified using multiple tagged primers as detailed on the ICoMM website at MBL (http://vamps.mbl.edu). Only sequences observed >10 times were considered for the analysis, and the operational taxonomic unit threshold of 3% was used. Samples

were compared with each other and to geochemical parameters using the Pearson's correlation coefficient function in Excel 2007.

Results

Geochemical gradients at different in-situ *temperatures*
The three push coring sites in Guaymas Basin showed distinct temperature and chemical gradients. Core 4483-23 at Mat Mound represented the cool temperature regime, increasing from 2 °C at the seawater/sediment interface almost linearly to *ca* 35 °C at 25 cm depth, without a further downcore increase (Figure 1 and Supplementary Table S2). Megamat core 4486-24 showed a steeper, almost linear temperature increase from *ca* 22 °C at 2 cm depth, toward 100 °C at 42 cm depth. At the hot UNC mat, the *in-situ* temperature at core 4489-11 increased exponentially toward 92–104 °C at 20 cm depth and then remained nearly constant in the 102–110 °C range toward 40 cm depth. Here, two temperature curves (T1 and T2) were measured that differ at the sediment surface, but converge toward 102–105 °C at 30 cm depth (Figure 1; Supplementary Table S2). The hotter temperature profile, with 57 °C at the sediment surface, was measured next to the cores 4489-10 and 11; the other profile was determined at a distance of 20 cm (Supplementary Figure S1).

Porewater concentration profiles and $\delta^{13}C$-isotopic signatures of methane provided consistent evidence of methanogenesis and AOM in Guaymas sediments. The methane porewater concentrations are affected by outgassing and bubble formation during core return to the surface. The methane content of the Guaymas hydrothermal fluids can reach at least 12 to 16 mM, two orders of magnitude higher than those of most bare lava vent sites (Welhan, 1988), and one order of magnitude above atmospheric saturation. The residual porewater methane concentrations that could be measured after retrieval of unpressurized cores were in the 1 to 5 mM range (Figure 1). The highest methane concentrations were found at the bottom of each core; they started to decrease conspicuously within *ca* 10 cm of the sediment surface, and continued to decrease toward the sediment surface (Figure 1).

Decreasing methane porewater concentrations coincided with the onset of ^{13}C-enrichment in methane at specific sediment depths. At the bottom of each core, methane has the lightest $\delta^{13}C$ signature, in the range of –35 to –45‰ (Figure 1). These results are similar to previously reported $\delta^{13}C$ values of −43 to −51‰ for Guaymas Basin methane (Welhan, 1988), which are interpreted as a mixed signature resulting from a smaller contribution of abiotic, thermocatalytic degradation of organic matter producing thermogenic methane ($\delta^{13}C = -20$ to −23‰) and a dominant proportion of biogenic methane (<−43.8‰) (Pearson *et al.*, 2005). Toward the sediment surface, methane becomes heavier ($\delta^{13}C = -26$ to −9‰), indicating preferential oxidation of ^{12}C-methane combined with selective retention of ^{13}C-methane. This trend begins at depths with distinctly different temperature regimes: at 8–10 cm sediment depth with an *in-situ* temperature of 15–20 °C in the cool core, at 6–8 cm and 30–35 °C in the warm core, and at 10–12 cm in the hot core (Figure 1). This sediment layer has an *in-situ* temperature range of 60–95 °C, depending on which of the two temperature profiles is applied (Figure 1).

The steepest change in $\delta^{13}C$ of methane occurs in the hot core, with over 30‰ difference between 13 and 5 cm depth; the two other sites show *ca* 10–15‰ difference over similar depth intervals (Figure 1). As accurate methane porewater concentrations remain to be determined with *in-situ* approaches (Wankel *et al.*, 2011), and advection rates for porewater fluids are not known, modeling of methane oxidation rates from methane concentration and $\delta^{13}C$ isotope profiles remains elusive. Yet, comparably steep methane concentration profiles from a Gulf of Mexico cold seep, from *ca* 2 mM methane maxima located near 10 cm depth to more than halved methane concentrations in the surficial 2 cm sediment layer, are accompanied by *ex-situ* rates of conversion of ^{14}C-labelled methane to ^{14}C-labelled CO_2 of $>100\,\mu M\,d^{-1}$ near the sediment surface (Lloyd *et al.*, 2010).

DIC concentrations are very high, in the range of 5–15 mM; they have a local maximum between 4 and 8 cm depth in cores 4483-23 and 4489-11, indicating active DIC-producing remineralization processes (Figure 1). The $\delta^{13}C$ signature of DIC is highly variable, between −5 and −25‰. The cool and the hot sediments show broad peaks of isotopically lighter DIC in the −20 to 25‰ range, consistent with the microbial remineralization of buried biomass of photosynthetic origin. A methane-derived contribution to DIC concentration peaks and isotopic signatures is likely for two reasons. Sediment horizons of light, $\delta^{13}C$-depleted DIC coincide with local maxima in DIC concentration, and both overlap with sediment horizons of isotopically heavy methane, a geochemical indicator for the oxidation of methane to CO_2. Also, the $\delta^{13}C$ signatures of porewater DIC at the cool and the hot site (minima at −23.18 and −20.93‰, respectively, Supplementary Table S2) are considerably lighter than those of hydrothermal DIC or deep subsurface DIC (Simoneit and Galimov, 1984; Peter and Shanks, 1992), an observation that is parsimoniously explained with a contribution of methane-derived carbon. For calcite chimney samples at Guaymas Basin, the chimney calcite $\delta^{13}C$ (−9.6 to 13.9‰) allowed calculation of the $\delta^{13}C$ of CO_2 in the hydrothermal fluids as −10.2‰ (Peter and Shanks, 1992), near the light endmember value of $\delta^{13}C$ in Guaymas vent fluid DIC, ranging from −1.5 to −10.5‰ (Whelan and Lupton, 1987). These $\delta^{13}C$-DIC signatures were interpreted as mixtures of the stable carbon isotopic composition of marine carbonates, mantle-derived DIC, and DIC resulting from decomposition of buried planktonic biomass (Peter and Shanks, 1992). A similar combination of biogenic and abiogenic contributions

was suggested as the most likely source for porewater DIC ($\delta^{13}C = -8.22$ to -16.43‰) in Guaymas deep subsurface sediments at Ocean Drilling Program site 477 (Simoneit and Galimov, 1984).

Interestingly, the warm sediment core shows heavier $\delta^{13}C$ values of DIC than the hot and cold cores, in the range of –10 to –15‰ (Figure 1), indicating a weaker methane-derived contribution to DIC than at the two other sites. This interpretation is consistent with the lower porewater methane concentrations at this site, and with the shallower depth (*ca* 8 cm) of the methane oxidation zone as reflected in ^{13}C-methane enrichment (Figure 1).

Porewater sulfate concentrations remained high (Figure 1), between 20 and 28 mM in the cool and hot cores or around 10 mM in the warm core. The persistent presence of porewater sulfate indicates lateral or vertical influx of seawater into the hydrothermally heated sediments at a faster rate than biological sulfate removal; this interpretation is consistent with previous microelectrode surveys of *Beggiatoa* mats showing periodical oxygen pulses within the mats and in sediments underneath (Gundersen *et al.*, 1992). Seawater intrusion during core recovery and outgassing is unlikely because porewater concentration and $\delta^{13}C$ profiles of methane and DIC are not flushed out. In multiple push core surveys of surficial sediments of Guaymas Basin, sulfate remained abundant at porewater concentrations of several mM (Jørgensen *et al.*, 1990; Elsgaard *et al.*, 1994; Weber and Jørgensen, 2002), suggesting that advective flux with sulfate admixture is a consistent feature of hydrothermally active Guaymas Basin sediments.

Porewater sulfide concentrations reach 1.8 mM in the cool core and 4.6 mM in the hot core at 5 to 7 cm depth. The same depth horizons of the warm core have much lower sulfide concentrations near the spectrophotometric detection limit (3 μM); downcore sulfide concentrations do not rise above the 0.3 mM range (Figure 1). The high sulfide concentrations in the cool and the hot core persist close to the sediment surface and decline only in the 0–1 cm sediment layer (Figure 1). The hot core shows a sudden drop in sulfide concentrations toward zero near the bottom of the core. This anomaly might indicate localized seawater admixture or sulfide reoxidation within the sediments; seawater flushing during core recovery is ruled out by the persistently high methane porewater concentrations. The steep rise in sulfate concentrations and drop in sulfide concentrations at the bottom of the cores have been observed previously at Guaymas Basin (Jørgensen *et al.*, 1990).

16S rRNA archaeal diversity

The distinct temperature regimes in the AOM zones, and the different geochemical regimes in the sediment cores, were compared with sequence-based surveys of microbial community structure in these cores and sediment layers. Two different primer sets for general archaea (A8F/A915R) and for Euryarchaeota (A8f/Eury 498R) amplified archaeal 16S rRNA gene sequences from the AOM zones in these three cores (Supplementary Table S1A). The archaeal 16S rRNA gene clone libraries for the cool, warm and hot AOM zones show significant differences (Supplementary Figures S3–5). The cool and hot AOM zones are dominated by archaeal phylotypes of the uncultured Miscellaneous Crenarchaeotal Group archaea, one of the most frequently recovered archaeal lineages in marine subsurface sediments (Fry *et al.*, 2008; Teske and Sørensen, 2008), by uncultured members of the Thermoproteales (Supplementary Figure S4), by ANME-1, and by relatives of thermophilic, mostly sulfate- and iron-reducing Archaeoglobales (Supplementary Figure S5).

In contrast, the archaeal 16S rRNA gene clone library from the warm AOM zone is dominated by the uncultured Marine Benthic Group D (Supplementary Figure S5), an uncultured archaeal lineage within the Thermoplasmatales that is often found in methane seep habitats, and also by ANME-2 archaea and other members of the Methanosarcinales (Figure 2). This archaeal community might be distinct because of the geochemical and physical characteristics of this hydrothermally active sediment: the lack or low concentrations of porewater sulfide at the cored sediment, the lower porewater methane concentrations, and the possibility for reduced bioremineralization of buried biomass and/or seawater admixture as reflected in heavy $\delta^{13}C$–DIC values, set it apart from all other sampled locations (Figure 1).

Phylogenetic analysis of the 16S rRNA genes of methanogenic and ANME archaea revealed a monophyletic subgroup of ANME-1 archaea consisting only of phylotypes found in Guaymas Basin; this lineage is therefore termed ANME-1Guaymas (Figure 2). This designation reflects phylogenetic affinity, and does not postulate an obligate methanotrophic metabolism, given that the environmental distribution and gene expression patterns of ANME-1 archaea indicate facultative methanogenic potential (Lloyd *et al.*, 2011; Bowles *et al.*, 2011). The ANME-1Guaymas group is distinct from other hydrothermal vent ANME-1 phylotypes, such as those from the Lost City hydrothermal vents (Figure 2). ANME-1Guaymas 16S rRNA gene sequences were found in both cool and hot cores. The ANME-1Guaymas clade was further confirmed by RNA extraction and RT-PCR amplification of the 16S rRNA genes, and dominated the rRNA-based clone libraries in the hot core (19 ANME-1Guaymas clones vs 5 ANME-1a clones).

Functional genes of methanogenesis and methane oxidation

Within the methanogenic and methane-oxidizing archaea, the *mcrA* gene has similar phylogenetic resolution as the 16S rRNA gene (see Luton *et al.*, 2002 for one of many case studies), and therefore permits

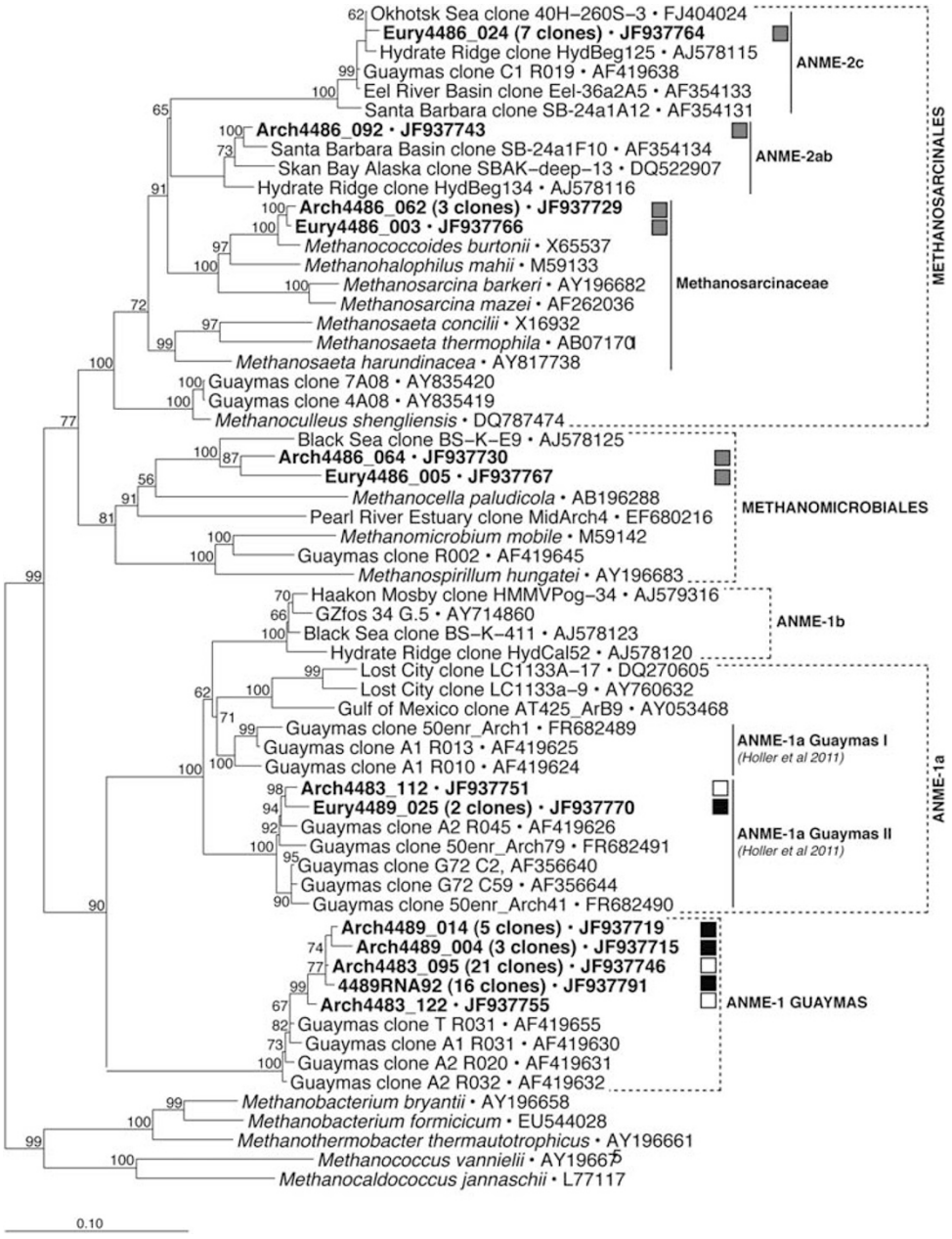

Figure 2 Archaeal 16S rRNA gene phylogeny of Guaymas Basin clones from hydrothermal sediment cores at 15–20 °C (open squares), 30–35 °C (grey squares) and 60–95 °C (black squares). Clones previously found at Guaymas Basin are included for context. rRNA clones are marked RNA in boldface, after the core number 4489. This neighbor-joining tree was constructed in ARB using 16S rRNA gene positions 28 to 915. Shorter clone sequences (marked EURY) were added subsequently without altering the tree topology. Bootstrap values over 50% based on 1000 replicates are shown.

an independent analysis of the methane-cycling archaeal community. In the hot and cool cores, *mcrA* genes formed a new Guaymas-specific monophyletic lineage (Figure 3), a sister lineage to the previously defined *mcrA* groups a and b that constitute the *mcrA* equivalent to the 16S rRNA-defined ANME-1 group (Hallam *et al*., 2003). As it is congruent with the monophyletic 16S rRNA lineage of ANME-1Guaymas archaea from the same sites, and is currently represented by Guaymas Basin clones only, it is termed mcrA-Guaymas (Figure 3). In addition to mcrA-Guaymas, the hot sediment core yielded *mcrA* group a (Hallam *et al*., 2003) (Figure 3). These phylotypes were found over several adjacent depth horizons and temperature horizons within the hot core, at 8 to 10 cm, 10 to 12 cm and 12 to 14 cm depth (Supplementary Table S2). This depth interval of 8 to 14 cm corresponded to a temperature range of approximately 85 °C to 100 °C in temperature profile T2, adjacent to the sediment core used for sequencing, and a temperature range of approximately 45 °C to 70 °C in temperature profile T1, *ca* 20 cm distant

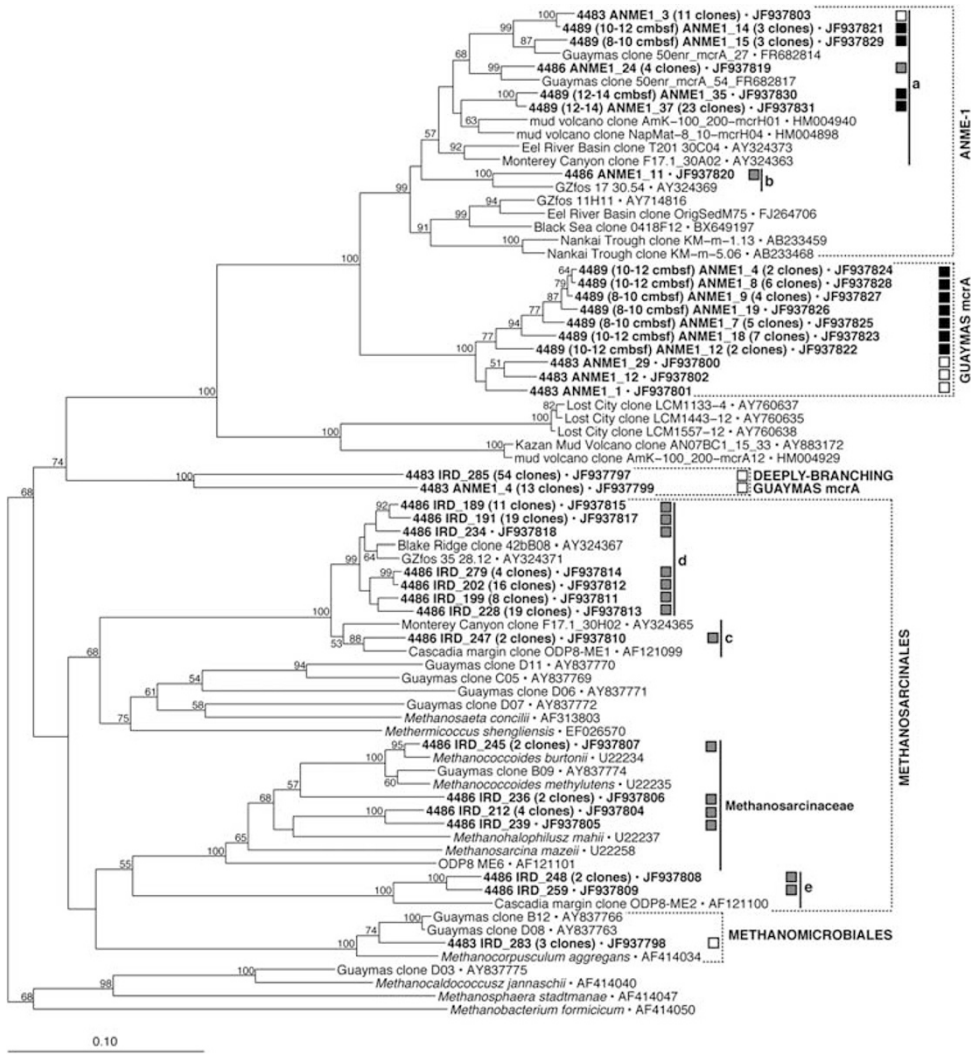

Figure 3 Neighbor-joining distance phylogeny of *mcrA* genes from Guaymas Basin hydrothermal sediment cores at 15–20 °C (open squares), 30–35 °C (grey squares) and 60–95 °C (black squares). Clones previously found at Guaymas Basin are included for context. Bootstrap values over 50% based on 1000 replicates are shown.

(Supplementary Figure S1C). Interestingly, mcrA a and mcrA-Guaymas were also detected in the AOM zone at the cool site, in addition to other *mcrA* genes: uncultured Methanomicrobiales clones formed a monophyletic lineage with *mcrA* clones from a previous Guaymas survey and the cultured species *Methanocorpusculum aggregans* (Dhillon *et al*., 2005) (Figure 3). Two *mcrA* clones from the cool core formed a new lineage that at present cannot be subsumed under any of the known families and genera of methanogens (Figure 3).

The *mcrA* genes obtained from the warm core represented the mcrA groups c and d, phylogenetically congruent with ANME-2, and mcrA group e, a distinct lineage within the Methanosarcinales (Hallam *et al*., 2003). The mcrA groups a and b, equivalent to ANME-1, were only detected with *mcrA* primers that are specific for this *mcrA* lineage (Lever, 2008); generic *mcrA* primers, or archaeal 16S rRNA primers and V6-tag primers did not detect ANME-1 archaea at this location.

These contrasting *mcrA* profiles between the hot and cool sediment on one hand, and the warm sediment on the other, are consistent with the results obtained with general archaeal 16S rRNA primers and with archaeal V6-tag sequencing primers. ANME-1 archaea dominate the hot and cool sites, but they constitute only a minor component of the methane-cycling archaeal community at the warm site that is dominated by members of the Methanosarcinales and ANME-2 archaea (Figure 3). These distinct methane-cycling archaeal communities may reflect other site-specific controls than temperature regime at the time of sampling, for example, geochemical characteristics, or temporal dynamics of fluctuating temperature and hydrothermal flow conditions that could not be monitored during short sampling visits.

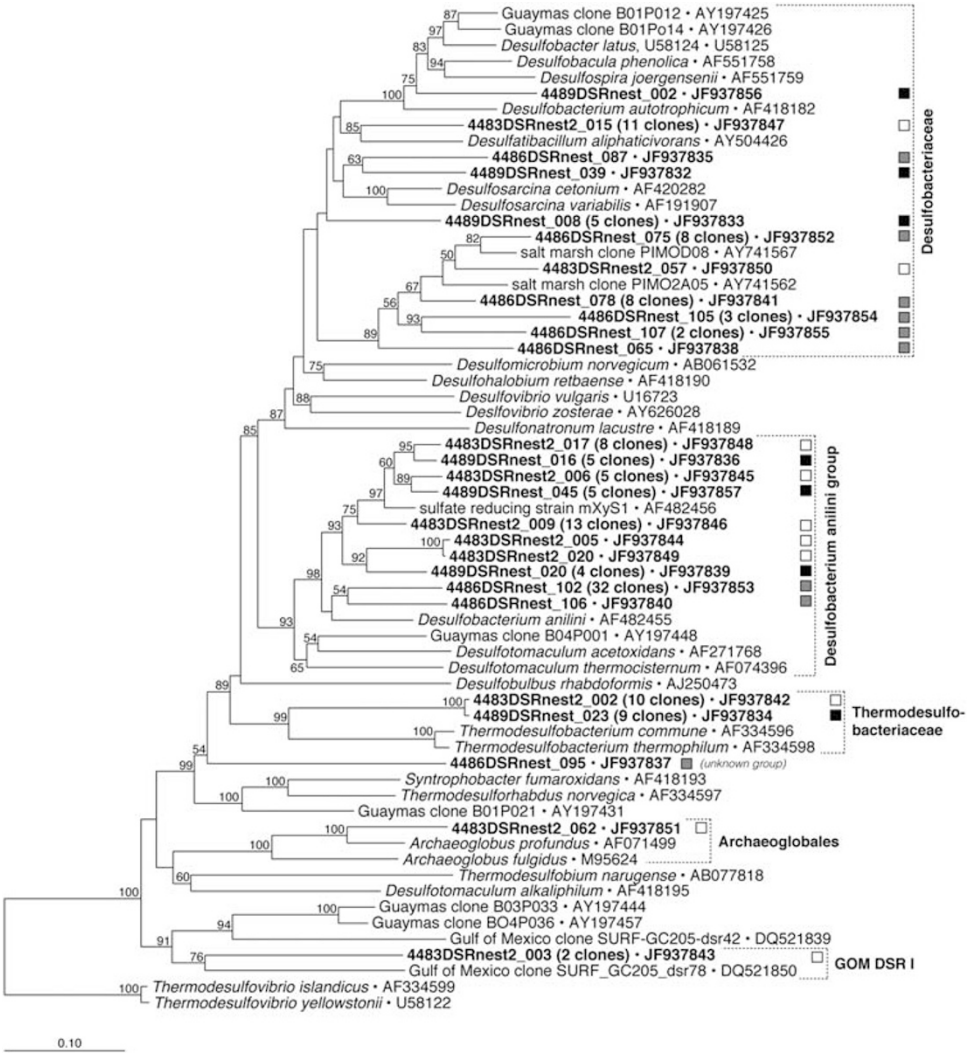

Figure 4 Neighbor-joining distance phylogeny of predicted amino acid translations of partial *dsrAB* genes from Guaymas Basin hydrothermal sediment cores at 15–20 °C (open squares), 30–35 °C (grey squares) and 60–95 °C (black squares). Clones previously found at Guaymas Basin are included for context. Bootstrap values over 50% based on 1000 replicates are shown.

Functional genes of sulfate reduction

From all three cores, *dsrAB* genes could be amplified and identified phylogenetically (Figure 4). Most *dsrAB* phylotypes were affiliated with deltaproteobacterial sulfate-reducing bacteria of the *Desulfobacterium anilini* group, specialists for the oxidation of aromatic hydrocarbons (Teske, 2010). The cultured representatives of this group oxidize some but not all of the aromatic carbon sources, such as xylene, alkyl benzenes, naphthalene, benzoate or phenylacetate (Kniemeyer *et al.*, 2003). Other clones are related to genera within the Desulfobacteriaceae, expanding the groups of sulfate-reducing bacteria and *dsrAB* genes that were previously found in Guaymas Basin (Dhillon *et al.*, 2003). At the cool Mat Mound site, clones of the Archaeoglobales were detected, a group that was missing in a previous *dsrAB* gene survey (Dhillon *et al.*, 2003) but strongly implied in rate measurements of sulfate reduction at hot temperatures in Guaymas Basin sediments. Clones of group IV, a frequently recovered marine sulfate reducer lineage at Guaymas and at cold seep sites (Dhillon *et al.*, 2003; Lloyd *et al.*, 2006), were not detected in this survey. Finally, *dsrAB* clones related to *Thermodesulfobacterium* were found at the cool and at the hot site (Figure 4).

V6-tag sequencing

To check the 16S rRNA clone library results against an alternative sequence analysis approach with several orders of magnitude higher sequence throughput, the same DNA extracts were subjected to tagged amplicon sequencing of the V6 region of the 16S rRNA gene. Using primer sets specific for bacterial and archaeal species, over 55 000 and 31 000 sequences were examined per sample, respectively (Figures 5a and b).

The V6 analysis suggests that different controls are placed on archaeal and bacterial communities as seen by the drastic shifts in community structure

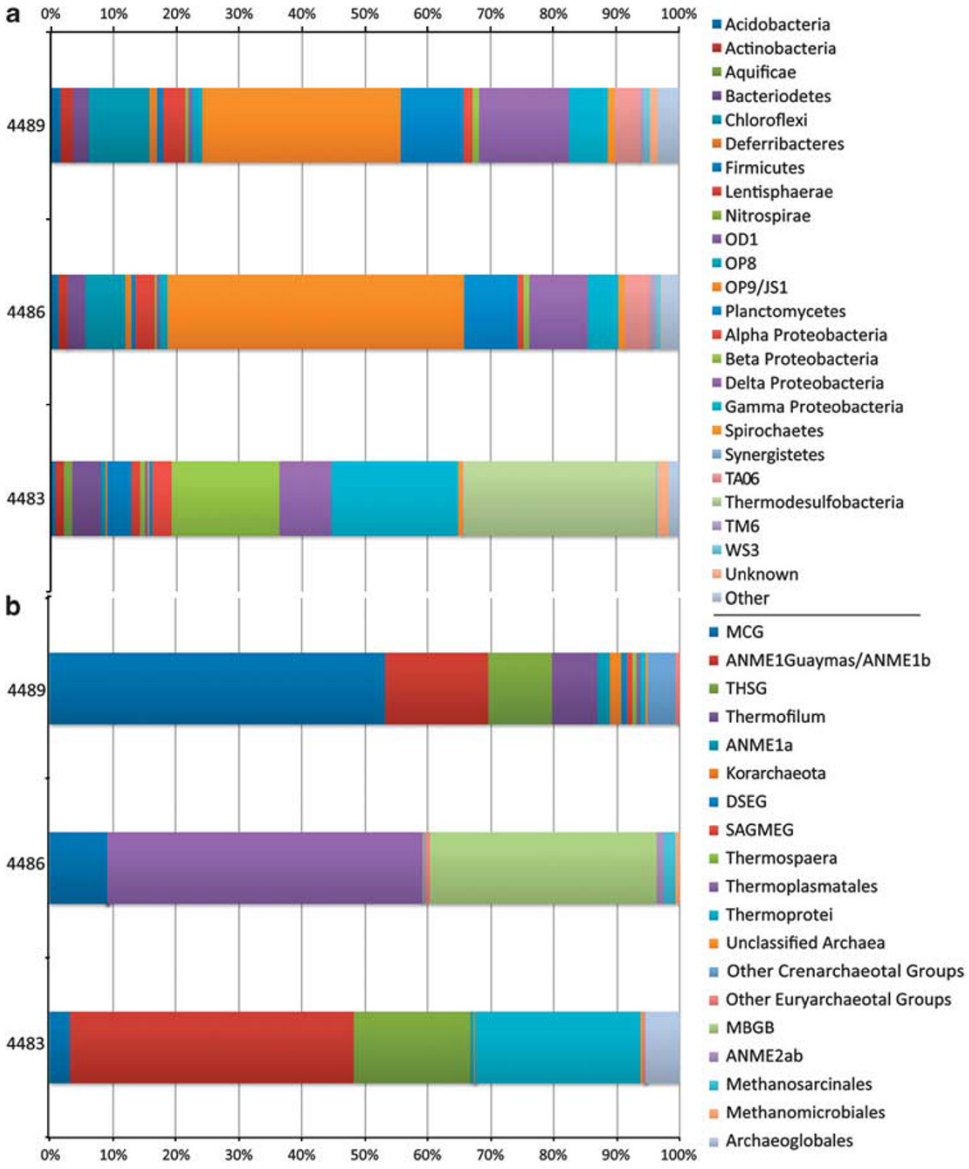

Figure 5 Bar charts of V6 tagged sequencing for (**a**) bacterial and (**b**) archaeal primer sets, for the hot, warm and cool sediment samples (cores 4489,10–12 cm; core 4486-22, 6–8 cm; and core 4483-21, 8–10 cm, respectively). The 100% bar corresponds to (**a**) 55 000 bacterial and (**b**) 31 000 archaeal sequences. Bacterial taxa represented by fewer than 300 V6-tag sequences are pooled as 'other'; these include the Caldiserica, Chlamydiae, Chlorobi, Cyanobacteria, Elusimicrobia, Fibrobacteres, Fusobacteria, Gemmatimonadetes, Epsilonproteobacteria, Tenericutes, Thermotogae, Verrucomicrobia, and the Candidate subdivisions OP1, OP10, OP11, OP2, OP3, TG-1 and WS-1.

between sites. Pearsons' correlations of taxon abundance, based on unique taxa identified at the phylum and subphylum level, show that bacterial phyla and subphyla are shared mostly between the warm and hot sediment cores ($r^2 = 0.959$) (Table 1a). This trend is driven by the predominance of the OP9 and JS1 candidate phyla at the warm and hot site, followed by the Chloroflexi and Planctomycetes (Figure 5a). The neighboring OP9 and JS1 lineages cannot be clearly distinguished in V6-tag analyses, and are therefore combined. The sister group relationship of these two bacterial lineages was already noted in the initial 16S rRNA analysis of the Guaymas sediments, when Guaymas phylotypes of the—yet unnamed—JS1 candidate phylum branched next to the OP9 candidate phylum (Teske *et al.*, 2002). The OP9, JS1, Chloroflexi and Planctomycetes are among the most frequently recovered bacterial phyla in the deep marine sedimentary subsurface (Teske, 2006; Fry *et al.*, 2008). In contrast, the cool sediment core is dominated by Thermodesulfobacteria, Betaproteobacteria and Gammaproteobacteria (Figure 5a). All sites contain Deltaproteobacteria; within this subphylum, the Desulfobacteriales include the sulfate-reducing syntrophs that physically associate with ANME archaea (Schreiber *et al.*, 2010) (Figure 5a).

Table 1 Pearson's correlations of (**a**) taxon abundances for pairwise combinations of cool (Mat Mound; core 4483-21), warm (Megamat, core 4486-22) and hot cores (UNC mat, core 4489-10), based on V6-tag bacterial and archaeal community composition and (**b**) temperature and porewater concentrations of methane, sulfate and sulfide with V6-tag abundances of Deltaproteobacteria, ANME-1Guaymas/1b, ANME-1a and ANME-2ab archaea

a

Comparison between two cores	*Correlation for bacterial communities*	*Correlation for archaeal communities*
Hot vs warm core	0.959	−0.195
Warm vs cool core	0.007	−0.166
Cool vs hot core	0.064	0.756

b

	Temperature	*Sulfate*	*Methane*	*Sulfide*
Deltaproteobacteria	0.933	0.780	0.082	0.290
ANME-1Guaymas/1b	−0.360	−0.917	0.844	0.713
ANME-1a	0.910	0.345	0.585	0.742
ANME-2ab	−0.305	0.463	−0.994	−0.995

A perfect positive linear correlation has a value of 1.0; a perfect negative linear correlation has a value of −1.0.

In contrast to the bacteria, the archaeal V6-tag results show the stronger taxon abundance correlations between the cool and the hot sites (Table 1a). The archaeal V6-tag profiles in the cool and hot sites are dominated by Miscellaneous Crenarchaeotal Group and ANME-1 archaea, although in strongly contrasting abundances; the warm site is dominated by members of the Marine Benthic Group B archaea and the Thermoplasmatales (Figure 5b). Consistent with the archaeal 16S rRNA clone libraries, no ANME-1 were seen in the warm core, and vice versa no ANME-2 were found in the cold and hot cores (Figure 5b), suggesting that site-specific geochemical controls and habitat characteristics separate these ANME groups. The V6 region cannot clearly differentiate the ANME-1Guaymas and ANME-1b lineages; both groups have been combined in the V6-tag analysis as ANME-1Guaymas because the 16S rRNA clone libraries lacked ANME-1b. These limitations show that nearly full-length PCR-amplified and sequenced 16S rRNA gene sequences remain indispensable for phylogenetic resolution and identification of novel lineages.

The microbial groups likely to be involved in AOM (Deltaproteobacteria, ANME-1Guaymas/1b, ANME-1a and ANME-2ab) were tested for correlation to temperature, and porewater concentrations of sulfate, methane and sulfide (Table 1b). Temperature appears to control the abundance of the Deltaproteobacteria and the ANME-1a group, but not the ANME-1 Guaymas/ANME-1b group, as previously suspected based on the 16S rRNA clone library results that had yielded ANME-1Guaymas phylotypes at the cool and at the hot site. Instead, the abundance of the ANME-1Guaymas/ANME-1b group correlates positively with high methane and negatively with high sulfate concentrations in the cool and hot cores, as evident also in the porewater profiles (Figure 1). Both ANME-1a and ANME-1Guaymas/ANME-1b groups correlate positively with sulfide concentrations. In contrast, ANME-2ab correlates negatively with sulfide and methane (Table 1b).

Discussion

Controls on ANME communities

In Guaymas Basin sediments, *in-situ* temperature controls on microbial community composition, especially ANME diversity, do not overrule the constraints of *in-situ* geochemical regimes, which appear to be at least as significant. In the hot and cold cores, sulfide reaches concentrations of 1–3 mM already in the 2 to 4 cm sediment layer; the sediments remain fully reduced throughout the sediment column, with the possible exception of the reoxidized bottom sediment of the hot core. In contrast, porewater sulfide remains near detection limit in the upper sediment layers of the warm core, and increases to above-background concentrations only at 10 cm depth and deeper downcore. Thus, the ANME-1 archaea in the cool and hot sediments inhabit a thoroughly reducing, strongly sulfidic sediment environment covered with sulfide-oxidizing *Beggiatoa* mats, whereas the ANME-2 archaea in the warm core exist in sediments with little or no free sulfide, and without *Beggiatoa* mat cover (Supplementary Figure S1). Similar changes in redox conditions in Gulf of Mexico cold seep sediments accompany a change in *Beggiatoa* mat cover and a change from ANME-1 to ANME-2 archaea (Lloyd *et al.*, 2010). Worldwide ANME archaeal lipid distributions in cool sediments and methane seeps have shown that ANME-1 are associated with more stably anoxic environments than are ANME-2 (Rossel *et al.*, 2011). These studies are consistent with our results showing ANME-1 correlating with sulfide (Table 1b).

High-temperature AOM

At Guaymas Basin, the potential for high-temperature AOM had been proposed (Teske *et al.*, 2002;

Schouten *et al.*, 2003; Kallmeyer and Boetius, 2004); *ex-situ* rate measurements in Guaymas sediments showed AOM activity between 35 °C to 87 °C (Kallmeyer and Boetius, 2004), and 15 °C to 70 °C, with maximal activity near 50 °C (Holler *et al.*, 2011). Here, isotopic, geochemical and molecular sediment profiles indicate active AOM at *in-situ* temperatures near 60 °C to 70 °C , if the temperature profiles are read conservatively, and into the range of 90 °C following the hotter of two relevant temperature profiles (Figure 1).

Ex-situ and *in-situ* AOM was associated with different archaeal communities. 16S rRNA and *mcrA* analysis of *ex-situ* incubations yielded members of the ANME-1a cluster and of the mcrA group a, respectively (Holler *et al.*, 2011). In contrast, sediments that were preserved at −80 °C immediately after sampling yielded also ANME-1Guaymas (Figure 2) and *mcrA*-Guaymas clones (Figure 3). This 16S and *mcrA* lineage cannot be subsumed under any other previously known clades, and are so far only found in hydrothermal sediments of Guaymas Basin. Both DNA and RNA sequencing show that the ANME-1 Guaymas archaea are present and active in sediment cores with *in-situ* temperature regimes of up to at least 70 °C. As this group was detected in sediments with *in-situ* temperatures as low as 20 °C and as high as >90 °C, the ANME-1Guaymas archaea are not necessarily obligate high-temperature specialists, but may represent eurythermal generalists that can withstand considerable fluctuations in temperature and hydrothermal flow.

Potential sulfate-reducing syntrophs

High-temperature sulfate-dependent AOM most likely require novel sulfate-reducing bacterial syntrophs. Interesting candidates are the members of the HotSeep-1 cluster, a deeply branching deltaproteobacterial lineage that was repeatedly found in hydrothermal Guaymas sediments. These bacteria were previously detected in near-surface Guaymas Basin sediments that harbor ANME-1Guaymas archaea (deltaproteobacterial clone A2B020; Teske *et al.*, 2002). They were subsequently found in n-butane-oxidizing sulfate-reducing enrichments from Guaymas sediment and called butane60 cluster (Kniemeyer *et al.*, 2007). They were detected again by fluorescence *in situ* hybridization and 16S rRNA gene sequencing in *ex-situ* high-temperature AOM enrichments from Guaymas Basin that showed the 1:1 stoichiometry of sulfate-dependent methane oxidation; their temperature preferences are most likely relevant for the overall temperature range of anaerobic methane oxidation (Holler *et al.*, 2011). In this survey, *dsrAB* phylotypes were affiliated with thermophilic and hyperthermophilic sulfate reducers of the genera *Thermodesulfobacterium* and *Archaeoglobus* (Figure 4). The 19 clones that constituted the *Thermodesulfobacterium*-related *dsrAB* lineage represented the third largest clone group after members of the Desulfobacteriaceae (38 clones) and the *Desulfobacterium anilini* group (74 clones). This *dsrAB* lineage remains to be linked to 16S rRNA phylogenies.

General relevance

High-temperature AOM vastly increases the global ecosystem space for microbial methanotrophy, not only at Guaymas Basin or in comparable high-temperature hydrocarbon seeps, but also in geothermally heated marine subsurface sediments (Roussel *et al.*, 2008), deep hydrocarbon reservoirs, or sedimented spreading centers, as in the Red Sea, the Gulf of Aden, the South China Sea, the Sea of Japan and the Aegean Sea. Anaerobic, sulfate-dependent methane oxidation can permeate a similar 'intraterrestrial' habitat space as other anaerobic microbial processes.

Acknowledgements

This study was supported by NSF Biological Oceanography (OCE-0647633) and by a Hansekolleg fellowship to AT, and by a NRC postdoctoral fellowship from the NASA Astrobiology Institute administered by ORAU to JFB. Further funding for this research was received by AB from the DFG (MARUM, University Bremen). The V6-tag pyrosequencing effort was supported by the International Census of Marine Microbes (ICoMM) at the Marine Biological Laboratory, Woods Hole. Dr Jesse Dillon (California State University, Long Beach) generously provided an alignment template for the *dsrAB* phylogeny. We thank the crew and pilots of RV Atlantis and HOV Alvin for their expert and unflagging support throughout the cruise, and all cruise participants and collaborators of Atlantis cruise AT-15-40 for their generous assistance, collegiality and unflappability at sea.

References

Albert DB, Martens CS. (1997). Determination of low-molecular weight organic acid concentrations in seawater and pore-water samples via HPLC. *Mar Chem* **56**: 27–37.

Bowles MW, Samarkin VA, Bowles KM, Joye SB. (2011). Weak coupling between sulfate reduction and the anaerobic oxidation of methane in methane-rich seafloor sediments during ex situ incubation. *Geochim Cosmochim Acta* **75**: 500–519.

Burggraff S, Mayer T, Amann R, Schadhauser S, Woese C, Stetter KO. (1994). Identifying members of the domain Archaea with rRNA-targeted oligonucleotide probes. *Appl Environ Microbiol* **60**: 3112–3119.

Cline JD. (1969). Spectrophotometric determination of hydrogen sulfide in natural waters. *Limnol Oceanog* **14**: 454–458.

Dhillon A, Lever M, Lloyd K, Albert DB, Sogin ML, Teske A. (2005). Methanogen diversity evidenced by molecular characterization of methyl coenzyme M reductase A (mcrA) genes in hydrothermal sediments of the Guaymas Basin. *Appl Environ Microbiol* **71**: 4592–4601.

Dhillon A, Teske A, Dillon J, Stahl D, Sogin ML. (2003). Molecular characterization of sulfate reducing bacteria

in the Guaymas Basin. *Appl Environ Microbiol* **69**: 2765–2772.

Elsgaard L, Isaksen MF, Jørgensen BB, Alayse AM, Jannasch HW. (1994). Microbial sulfate reduction in deep-sea sediments at the Guaymas Basin hydrothermal vent area: Influence of temperature and substrates. *Geochim Cosmochim Acta* **58**: 3335–3343.

Fry JC, Parkes RJ, Cragg BA, Weightman AJ, Webster G. (2008). Prokaryotic biodiversity and activity in the deep subseafloor biosphere. *FEMS Microbiol Ecol* **66**: 181–196.

Gundersen JK, Jørgensen BB, Larsen E, Jannasch HW. (1992). Mats of giant sulfur bacteria on deep-sea sediments due to fluctuation hydrothermal flow. *Nature* **360**: 454–455.

Hales BA, Edwards C, Ritchie DA, Hall G, Pickup RW *et al.* (1996). Isolation and identification of methanogen-specific DNA from blanket bog peat by PCR amplification. *Appl Environ Microbiol* **62**: 668–675.

Hallam SJ, Girguis PR, Preston CM, Richardson PM, DeLong EF. (2003). Identification of methyl coenzyme M reductase A (*mcrA*) genes associated with methane-oxidizing archaea. *Appl Environ Microbiol* **69**: 5483–5491.

Holler T, Widdel F, Knittel K, Amann R, Kellermann MY, Hinrichs KU *et al.* (2011). Thermophilic anaerobic oxidation of methane by marine microbial consortia. *ISME J*; e-pub ahead of print 23 June 2011; doi 10.1038/ismej.2011.77.

Islam T, Jensen S, Reigstad LJ, Larsen ∅, Birkelund N-K. (2008). Methane oxidation at 55 °C and pH 2 by a thermoacidophilic bacterium belonging to the Verrucomicrobia phylum. *Proc Natl Acad Sci USA* **105**: 300–304.

Jørgensen BB, Zawacki LX, Jannasch HW. (1990). Thermophilic bacterial sulfate reduction in deep-sea sediments at the Guaymas Basin hydrothermal vent site (Gulf of California). *Deep-Sea Res I* **37**: 695–710.

Kallmeyer J, Boetius A. (2004). Effects of temperature and pressure on sulfate reduction and anaerobic oxidation of methane in hydrothermal sediments of Guaymas Basin. *Appl Environ Microbiol* **70**: 1231–1233.

Kniemeyer O, Fischer T, Wilkes H, Glöckner FO, Widdel F. (2003). Anaerobic degradation of ethylbenzene by a new type of marine sulfate-reducing bacterium. *Appl Environ Microbiol* **69**: 760–768.

Kniemeyer O, Musat F, Sievert SM, Knittel K, Wilkes H, Blumenberg M *et al.* (2007). Anaerobic oxidation of short-chain hydrocarbons by marine sulphate-reducing bacteria. *Nature* **449**: 898–901.

Knittel K, Boetius A. (2009). Anaerobic oxidation of methane: progress with an unknown process. *Ann Rev Microbiol* **63**: 311–334.

Lever MA. (2008). *Anaerobic Carbon Cycling Pathways in the Subseafloor Investigated via Functional Genes, Chemical Gradients, Stable Carbon Isotopes, and Thermo-Dynamic Calculations*. The University of North Carolina at Chapel Hill: Chapel Hill, NC, USA, p. 145.

Lloyd KG, Albert DB, Biddle JF, Chanton J, Pizarro O, Teske A. (2010). Spatial structure and activity of sedimentary microbial communities underlying a *Beggiatoa spp*. mat in a Gulf of Mexico hydrocarbon seep. *PLoS One* **5**: e8738.

Lloyd KG, Alperin MJ, Teske A. (2011). Environmental evidence for net methane production and oxidation in putative ANaerobic MEthanotrophic (ANME) archaea. *Environ Microbiol* **13**: 2548–2564.

Lloyd KG, Lapham L, Teske A. (2006). An anaerobic methane-oxidizing community of ANME-1b archaea in hypersaline Gulf of Mexico sediments. *Appl Environ Microbiol* **72**: 7218–7230.

Ludwig W, Strunk O, Westram R, Richter L, Meier H, Yadhukumar K *et al.* (2004). ARB: a software environment for sequence data. *Nucleic Acids Res* **32**: 1363–1371.

Luton PE, Wayne JM, Sharp RJ, Riley PW. (2002). The *mcrA* gene as an alternative to 16S rRNA in the phylogenetic analysis of methanogen populations in landfill. *Microbiology* **148**: 3521–3530.

Martens CS. (1990). Generation of short chain organic acid anions in hydrothermally altered sediments of the Guaymas Basin, Gulf of California. *Appl Geochem* **5**: 71–76.

Martens CS, Albert DB, Alperin MJ. (1999). Stable isotope tracing of anaerobic methane oxidation in the gassy sediments of Eckernförde Bay, German Baltic Sea. *Am J Sci* **299**: 589–610.

Pearson A, Seewald JS, Eglinton TI. (2005). Bacterial incorporation of relict carbon in the hydrothermal environment of Guaymas Basin. *Geochim Cosmochim Acta* **69**: 5477–5486.

Peter JM, Shanks III WC. (1992). Sulfur, carbon and oxygen isotope variations in submarine hydrothermal deposits of Guaymas Basin, Gulf of California. *Geochim Cosmochim Acta* **56**: 2025–2040.

Reeburgh WS. (2007). Ocean methane biogeochemistry. *Chem Rev* **107**: 486–513.

Rossel PE, Elvert M, Ramette A, Boetius A, Hinrichs KU. (2011). Factors controlling the distribution of anaerobic methanotrophic communities in marine environments: Evidence from intact polar membrane lipids. *Geochim Cosmochim Acta* **75**: 164–184.

Roussel EG, Bonavita M-AC, Querellou J, Cragg BA, Webster G, Prieur D *et al.* (2008). Extending the subsea-floor biosphere. *Science* **320**: 1046.

Schreiber L, Holler T, Knittel K, Meyerdierks A, Amann R. (2010). Identification of the dominant sulfate-reducing bacterial partner of anaerobic methanotrophs of the ANME-2 clade. *Environ Microbiol* **12**: 2327–2340.

Schouten S, SWakeham SG, Hopmans EC, Sinninghe Damsté JS. (2003). Biogeochemical evidence that thermophilic archaea mediate the anaerobic oxidation of methane. *Appl Environ Microbiol* **69**: 1680–1686.

Simoneit BRT, Galimov EM. (1984). Geochemistry of interstitial gases in quaternary sediments of the Gulf of California. *Chem Geol* **43**: 151–166.

Springer E, Sachs MS, Woese CR, Boone DR. (1995). Partial gene sequences for the A subunit of methylcoenzyme M reductase (mcrI) as a phylogenetic tool for the family *Methanosarcinaceae*. *Intl J Syst Bacteriol* **45**: 554–559.

Swofford DL. (2000). *PAUP*. Phylogenetic Analysis Using Parsimony (and Other Methods)*, version 4.0b10. Sinauer Associates: Sunderland, MA.

Teske A. (2006). Microbial communities of deep marine subsurface sediments: molecular and cultivation surveys. *Geomicrobiol J* **23**: 357–368.

Teske A. (2010). Sulfate-reducing and methanogenic hydrocarbon-oxidizing microbial communities in the marine environment. Part 21: microbial communities based on hydrocarbons, oils and fats: natural habitats. In: Timmis K (ed). *Handbook of Hydrocarbon Microbiology*. Springer: Berlin, Heidelberg, pp 2203–2223.

Teske A, Hinrichs KU, Edgcomb V, de Vera Gomez A, Kysela D, Sylva SP *et al.* (2002). Microbial diversity of hydrothermal sediments in the Guaymas Basin: evidence for anaerobic methanotrophic communities. *Appl Environ Microbiol* **68**: 1994–2007.

Teske A, Sørensen KB. (2008). Uncultured archaea in deep marine subsurface sediments: have we caught them all? *ISME J* **2**: 3–18.

Wagner M, Roger AJ, Flax JL, Brusseau GA, Stahl DA. (1998). Phylogeny of dissimilatory sulfite reductases supports an early origin of sulfate respiration. *J Bacteriol* **180**: 2975–2982.

Wankel SD, Joye SB, Samarkin VA, Shah S, Friderich G, Melas-Kryiazi J *et al.* (2011). New constraints on diffusive methane fluxes and rates of anaerobic methane oxidation in a Gulf of Mexico brine pool through the use of a deep sea *in situ* mass spectrometer. *Deep Sea Res II* **57**: 2022–2029.

Weber A, Jørgensen BB. (2002). Bacterial sulfate reduction in hydrothermal sediments of the Guaymas Basin, Gulf of California, Mexico. *Deep-Sea Res I* **49**: 827–841.

Welhan JA. (1988). Origins of methane in hydrothermal systems. *Chem Geol* **71**: 183–1988.

Whelan JA, Lupton JE. (1987). Light hydrocarbon gases in Guaymas Basin hydrothermal fluids: Thermogenic versus abiogenic origin. *Amer Assoc Petrol Geol Bull* **71**: 215–223.

Supplementary Information accompanies the paper on The ISME Journal website (http://www.nature.com/ismej)